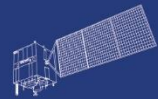


HY



HJ-1AB



CBERS



Gaofen



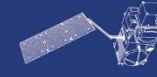
Beijing-2



Sentinel-1



Sentinel-2



Sentinel-3



Sentinel-5p



Aeolus

**2023 DRAGON 5 3<sup>rd</sup> YEAR RESULTS SYMPOSIUM**

**YOUNG SCIENTISTS POSTER SESSION**

**12 SEPTEMBER 2023**

**[PROJECT ID. 59236]**

**[THE CROSS-CALIBRATION AND  
VALIDATION OF CSES/SWARM MAGNETIC  
FIELD AND PLASMA DATA]**

- Dragon 5 project id: 59236
- Poster Title: An Improved In-Flight Calibration Scheme for CSES Magnetic Field Data
- Authors: Yang, Yanyan; Zeren, Zhima; Shen, Xuhui; Wang, Jie; Zhou, Bin; Lu, Hengxin; Guo, Feng; Magnes, Werner; Pollinger, Andreas; Miao, Yuanqing
- Presented by: [Yanyan Yang]

## Objectives

- To carry out in-flight calibration of CSES magnetic field
- To develop and optimize CSES magnetic field data processing

## Research Approach (including EO and other data)

- **Scalar calibration of FGM intrinsic parameters**

Magnetic field vectors in orthogonal and non-orthogonal FGM sensor frame  $\mathbf{B}_{\text{orth}}$  and  $\mathbf{B}_{\text{non-orth}}$  are related as follows:

$$\mathbf{B}_{\text{orth}} = \underline{\underline{\mathbf{P}}}^{-1} \cdot \underline{\underline{\mathbf{S}}}^{-1} \cdot (\mathbf{B}_{\text{non-orth}} - \mathbf{b})$$

Non-orthogonality    Scale value    Offsets

$$F_{FGM} = |\mathbf{B}_{\text{orth}}| = \sqrt{\mathbf{B}_{\text{orth}}^T \cdot \mathbf{B}_{\text{orth}}}$$

$$= \sqrt{[\underline{\underline{\mathbf{P}}}^{-1} \cdot \underline{\underline{\mathbf{S}}}^{-1} \cdot (\mathbf{B}_{\text{non-orth}} - \mathbf{b})]^T \cdot \underline{\underline{\mathbf{P}}}^{-1} \cdot \underline{\underline{\mathbf{S}}}^{-1} \cdot (\mathbf{B}_{\text{non-orth}} - \mathbf{b})}$$

**Model parameters to be solved**  $\mathbf{m} = (b_{0,i}, b_{s,i}, S_{0,i}, S_{s,i}, u_i)$

$$\mathbf{m}^{i+1} = \mathbf{m}^i + \delta \mathbf{m}^i$$

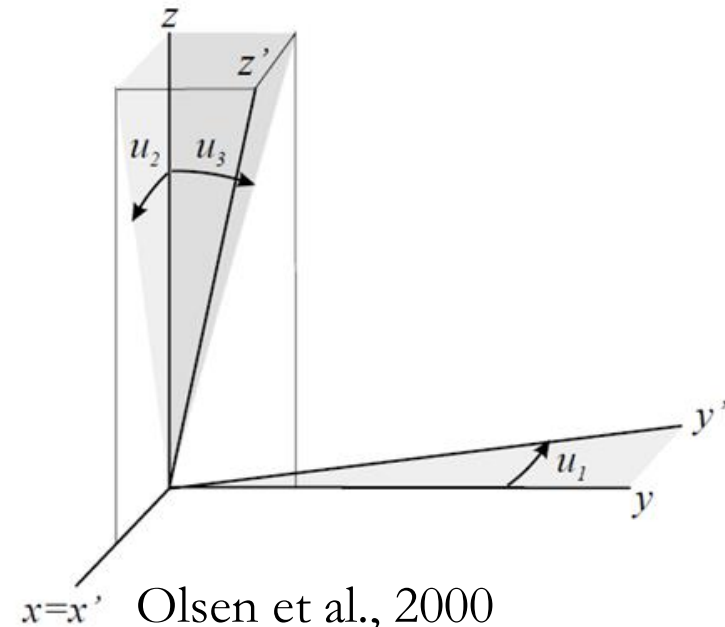
Iteratively linearized

robust LS approach  $\delta \mathbf{m}^i = [(\underline{\underline{\mathbf{G}}}^i)^T \cdot \underline{\underline{\mathbf{W}}}^i \cdot \underline{\underline{\mathbf{G}}}^i + \underline{\underline{\mathbf{W}}}^i_p]^{-1} \cdot [(\underline{\underline{\mathbf{G}}}^i)^T \cdot \underline{\underline{\mathbf{W}}}^i \cdot \delta \mathbf{d}^i + \underline{\underline{\mathbf{W}}}^i_p \cdot (\mathbf{m}^i - \mathbf{m}_p)]$

Further temperature correction

$$S_i = S_{0,i} + S_{s,i} T_s$$

$$b_i = b_{0,i} + b_{s,i} T_s$$

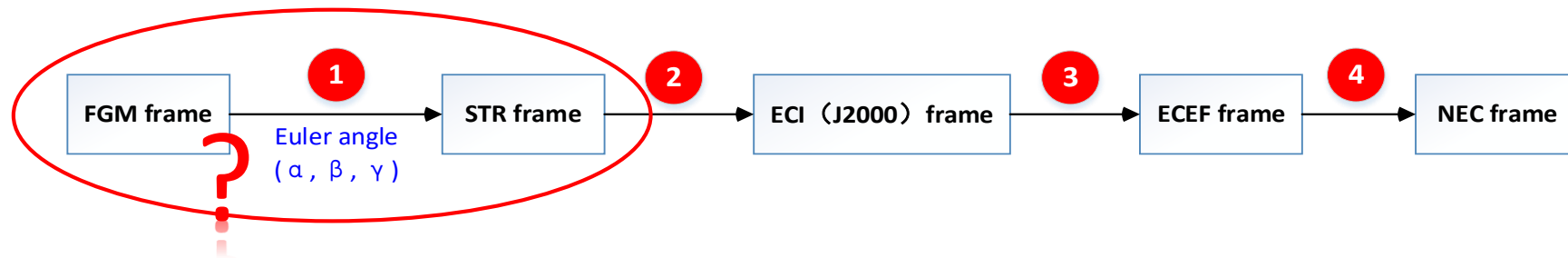


## Research Approach (including EO and other data)

- **Alignment of FGM along with global geomagnetic field modelling**

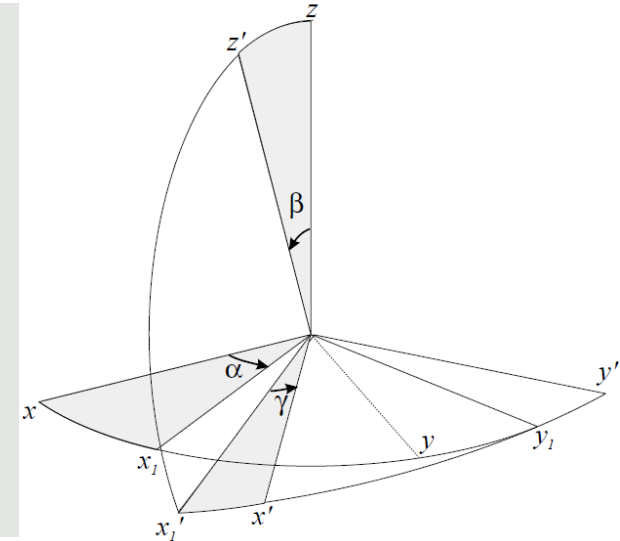
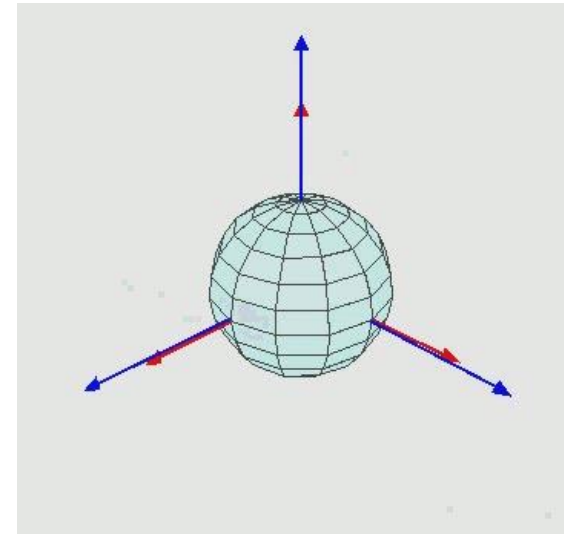
Euler angles: describe rotation of two coordinate systems.

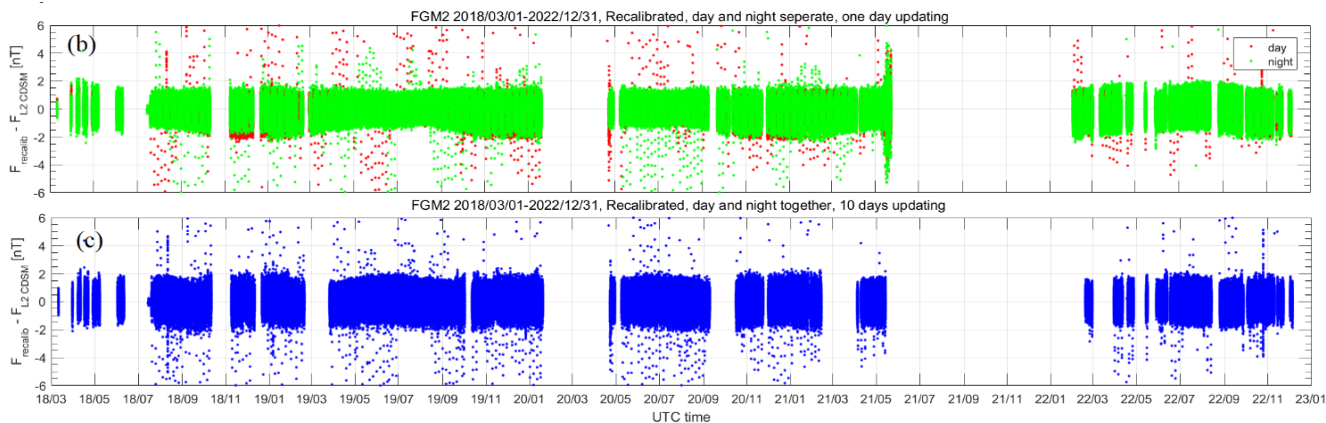
Will be solved along with the Gauss coefficients of a global geomagnetic field model



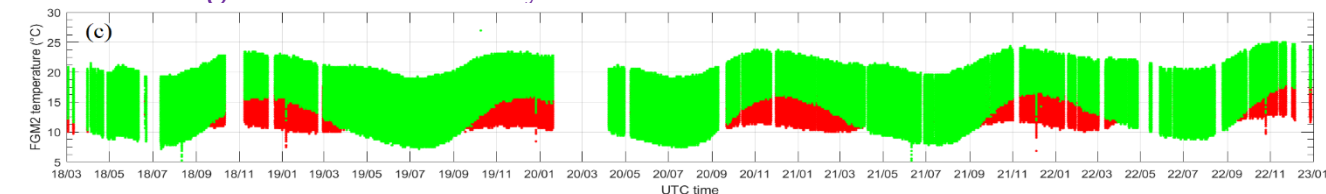
$$\mathbf{B}_{NEC} = R_{ECEF2NEC} R_{ECI2ECEF} R_{STR2ECI} R_{FGM2STR} \mathbf{B}_{FGM}$$

$$R_{FGM2STR}(\alpha, \beta, \gamma) = \begin{pmatrix} 0 & 0 & 1 \\ 1 & 0 & 0 \\ 0 & 1 & 0 \end{pmatrix} \begin{pmatrix} \cos\gamma & -\sin\gamma & 0 \\ \sin\gamma & \cos\gamma & 0 \\ 0 & 0 & 1 \end{pmatrix} \begin{pmatrix} \cos\beta & 0 & \sin\beta \\ 0 & 1 & 0 \\ -\sin\beta & 0 & \cos\beta \end{pmatrix} \begin{pmatrix} 1 & 0 & 0 \\ 0 & \cos\alpha & -\sin\alpha \\ 0 & \sin\alpha & \cos\alpha \end{pmatrix}$$

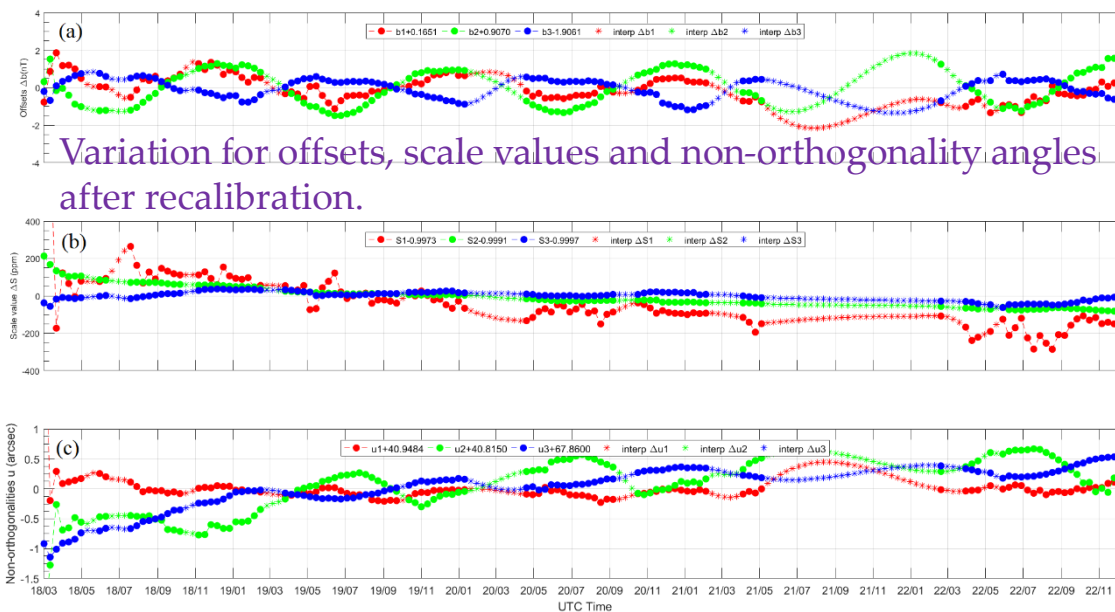




The magnetic field intensity residual before and after recalibration



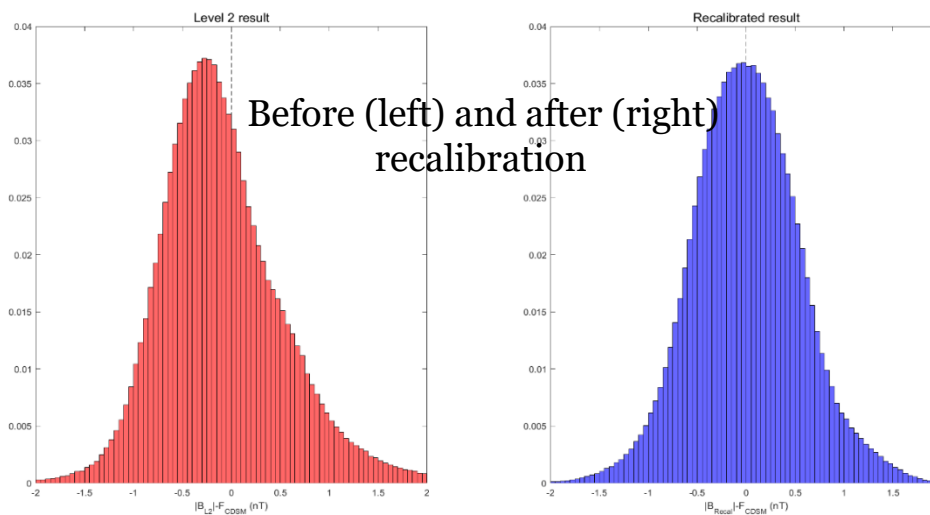
The temperature variation of FGM sensor



## Main optimization of the calibration procedures:

- Further consider temperature correction for the offsets and the scale factors
- Prolong the updating period of the calibration parameters from one day to 10 days (and without dayside and nightside data separation)

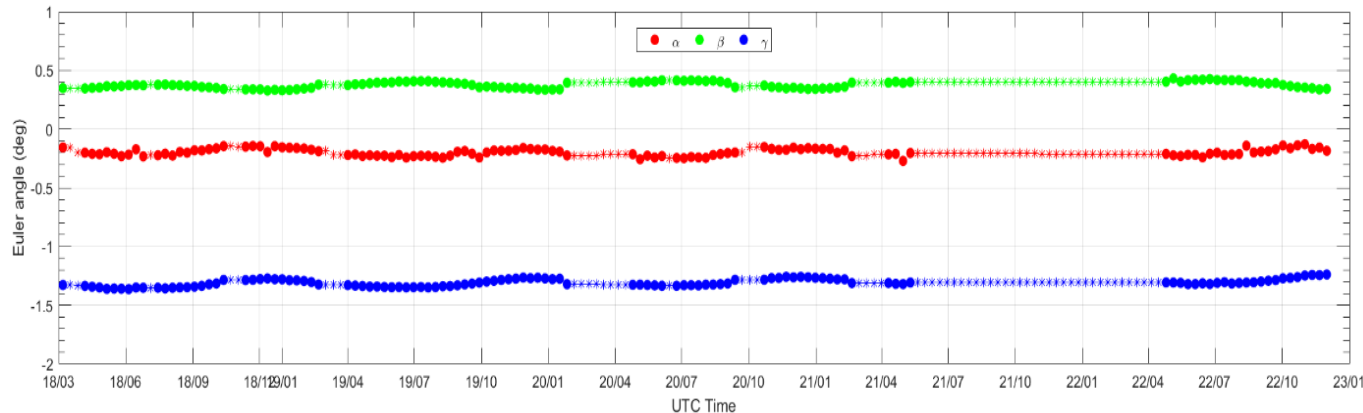
The typical variation is  $\pm 2\text{nT}$  for the offsets, less than 200 ppm (most of the time is less than 100 ppm) for the scale values and  $\pm 0.0002$  deg (about 0.7 arcsecs) for the non-orthogonality angles.



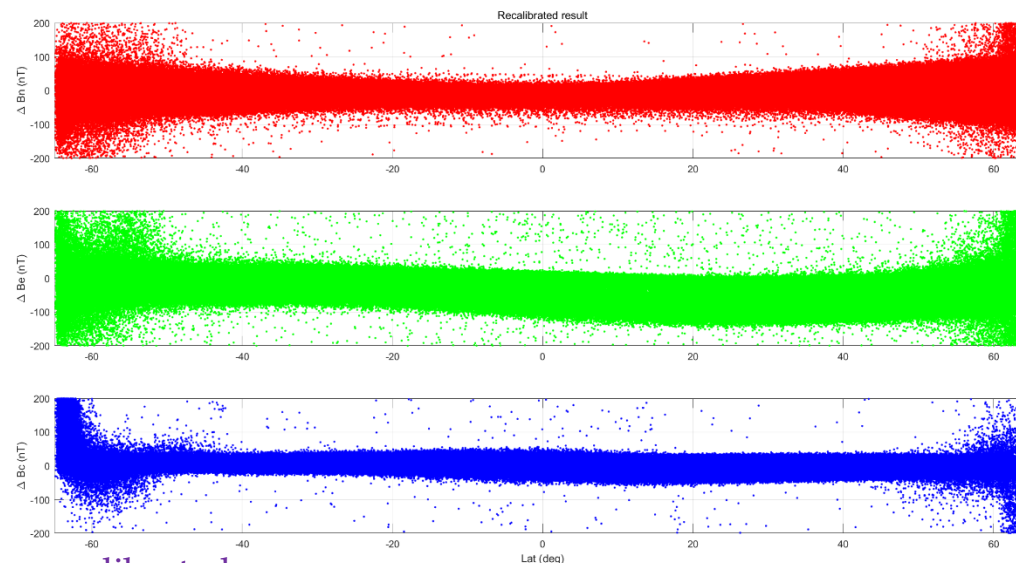
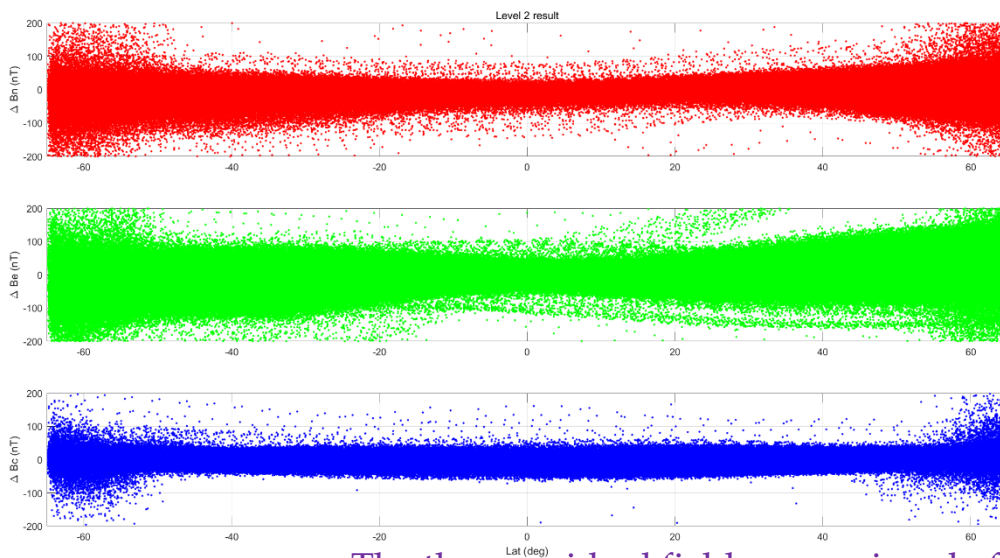
After the recalibration, the residuals become more standard Gaussian and more central distributed. For about 93% datasets, the residual field is less than 1nT.

## Main optimization of the calibration procedures:

- Solve the Euler angles along with global geomagnetic field modeling, no longer depend on other geomagnetic field models
- Extend the updating period of Euler angles from one day to 10 days
- When there is no CDSM data, the alignment of FGM is still possible by interpolation of model parameters.



The variation of in-orbit estimated three Euler angles for the alignment of the FGM sensor



The three residual field comparison before and after recalibrated

In the new calibration scheme, the latitudinal trend for the east component is improved to some extent.

## Conclusions

- **After rechecking almost all years data, it has become possible to make an improvement to the in-flight calibration of CSES magnetic field data.**
- **FGM sensor temperature correction on offsets and scale values have been taken into account to remove seasonal effects.**
- **Euler angles have been estimated along with global geomagnetic field modeling to improve the alignment of the FGM sensor.**
- **It has become possible to prolong the updating period of all calibration parameters from daily to 10 days, without the separation of dayside and nightside data.**
- **The new algorithms can optimize routine CSES magnetic field data processing efficiency and data quality.**

- Key references

- An Improved In-Flight Calibration Scheme for CSES Magnetic Field Data, Remote sensing, under review
- Olsen N et al (2003) Calibration of the Ørsted vector magnetometer. Earth Planets Space 55:11–18
- Tøffner-Clausen L, Lesur V, Olsen N, Finlay CC (2016) In-flight scalar calibration and characterisation of the Swarm magnetometry package. Earth Planets Space 68(1):129. <https://doi.org/10.1186/s40623-016-0501-6>
- Yin F, Lüher H (2011) Recalibration of the CHAMP satellite magnetic field measurements. Meas Sci Technol 22(5):055,101

- Acknowledgements

- This work makes use of the data from the CSES mission (<https://www.leos.ac.cn>).
- This work was supported by Dragon 5 cooperation 2020-2024 (project no. 59236), NSFC Grant Nos. 42274214, 41904134 and 42004051 and the APSCO Earthquake Research Project Phase II